

Industry Sector	RTD Thematic Area	Date
Civil Construction & Marine and Offshore	Durability and Life Extension	

## Simulation of local damage in ship to ship collision

K. Wisniewski, P. Kolakowski, B. Rozmarynowski, J.T. Gierlinski

WS Atkins Consultants, Epsom, United Kingdom

### Summary:

The paper presents results of numerical simulations of the local behaviour of a struck ship during a collision of two vessels. The struck vessel is a 105400 DWT double hull crude oil carrier, while the striking ship is a 40000 DWT container vessel with a bulbous bow, modelled as a rigid body. The dynamic analysis has been performed using the FE code ABAQUS-Explicit, which allowed to monitor the deformation and damage progression in time, accounting for large plastic strains and including the contact between the ships. To investigate sensitivity of the damage with respect to several parameters, such as : the material model, the friction coefficient for the contact between the vessels and the initial velocity of the striking ship, a number of parametric studies has been carried out.

## 1 Introduction

The results presented in the present paper were obtained within the project HARDER, which is concerned with development of new, harmonized rules for probabilistic assessment of damaged ship survivability. Current guidelines of maritime organizations are shifting from prescribed rules towards a more rational safety verification of individual ships, and hence it becomes important to establish a relationship between the features of the colliding ships and the resulting extent of damage, for various collision scenarios. This could be done using efficient, yet sufficiently accurate tools of structural analyses, such as e.g. a dynamic FE code ABAQUS-Explicit applied in the present computations. Such codes not only allow to model the geometry and structural parts of colliding ships quite accurately, but also are capable to deal with non-linear phenomena, such as crushing and tearing of the material, while simultaneously accounting for an in time change of contact between the colliding ships.

As proposed by Minorsky in 1959, a collision problem often is split into the so-called external dynamics and the internal mechanics, where the first one is concerned with the global ships motion, while the second with the energy absorbed by the ships. The external dynamics typically involves several simplifications, see e.g. by Pedersen and Zhang [ref. 2], such as: (a) only the dominant types of motion are considered, (b) the surrounding water is modeled by the added mass, and (c) the configuration of vessels remains constant during the event. A more computer-oriented approach is presented in Lenselink and Thung [ref. 1], and it is divided into 3 steps: (1) structure-structure collision calculations without the influence of the water, (2) water resistance calculations for a rigid motion of the struck ship, and (3) the combined fluid-structure calculations. It was found there that about 20% of the initial kinetic energy was dissipated by the water.

The present paper is concerned with the so-called internal mechanics of collision. Despite the earlier validation effort, e.g. of Wierzbicki [ref. 6], Lenselink and Thung [ref. 1], Wierzbicki [ref. 7] and Simonsen and Ockali [ref. 4], it has been considered desirable to perform further comparisons using realistic ship collision scenarios. The analyses have been tailored to assess the influence on the double-hull ship response of the following features of the model: (i) the material model, (ii) the friction coefficient for the contact between vessels, (iii) the initial velocity of the striking ship, and (iv) the mass scaling option used to accelerate computations.

In Section 2 the geometry of the ships participating in collision is defined. In Section 3 the finite element models of the ships and the material data are described. Section 4 presents numerical analyses and reference results obtained in this work. Section 5 shows comparisons for selected parameters, while discussion of the obtained results is presented in Section 6.

## 2 Geometry of ships participating in collision

The data for ships in collision have been obtained under the HARDER project. The struck ship is a 105 400 DWT double hull crude oil carrier, for which the main data is as follows:

Length	234.0 m,
Breadth	42.0 m,
Depth	21.0 m,
Draught	14.9 m,
Displacement	122 870 t.

The striking ship is a 40 000 DWT container vessel, with the bow consisting of a conventional bow and a bulbous bow. The data for this ship is as follows:

Length	211.5 m,
Breadth	32.2 m,
Depth	24.0 m,
Draught	11.9 m,
Displacement	54 000 t,

Stem angle  $61.5^{\circ}$ ,

where for the bulbous bow we assumed:

Length	7.5	m,
Vertical span	10.2	m,
Horizontal span	5.0	m.

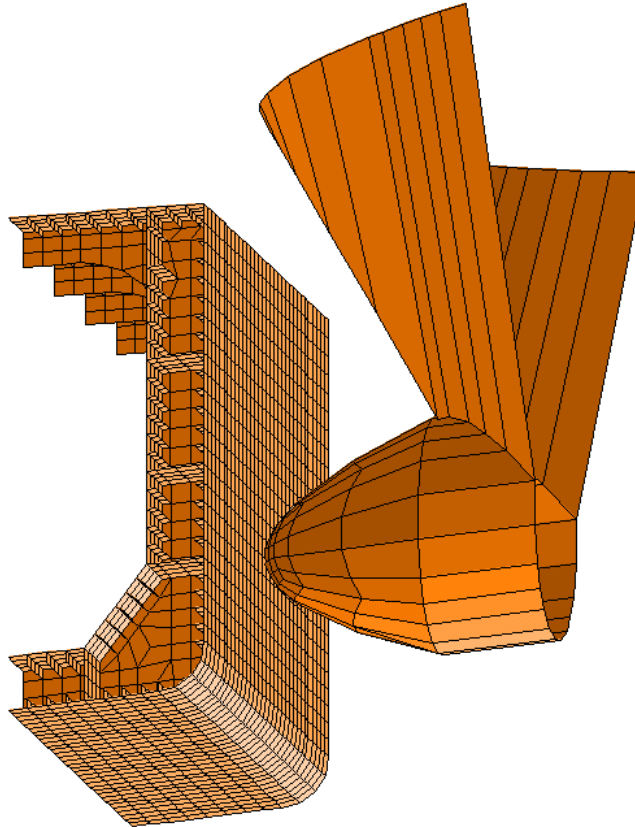


Fig. 1: Geometry and relative position of colliding ships

The collision scenario assumed that the ships collided at the angle of 90 degrees. The struck ship was stationary, while the striking ship was moving. Only a horizontal forward motion of the striking ship was allowed, and its initial velocity in the direction perpendicular to the struck ship was set to 7 knots (3.6 m/sec). The crude oil carrier was hit by the container vessel, in the middle between two web frames located near the mid-ship section (see Fig. 1).

### 3 FE models of ships

#### 3.1 Model of the bow of striking ship

The striking ship has been modelled as a rigid body. The FE model of the bow consists of 148 nodes, and 134 rigid finite elements, of which 124 are 4-noded, and 10 are 3-noded. Because the used elements are rigid hence it has not been necessary to keep the element aspect ratio at about 1.0; the only aim has been to provide a good representation of the modelled geometry.

### 3.2 Model of the struck ship

As mentioned earlier, the middle part of the struck ship has been selected for the FE modelling. The FE model has been generated using the FEMGV software. The geometrical data have been obtained from technical drawings of the struck ship. The model consists of 5132 nodes and 5512 shell finite elements, predominantly 4-noded, with 28 of them 3-noded.

The number of the degrees of freedom for the struck ship is 30792. In a direction perpendicular to the ship axis, approximately a quarter of the deck and a quarter of the bottom of the ship's hull has been modelled. The modelled part of the struck ship consists of 8 structural groups: frames, outer hull plating, deck, inner hull plating, outer hull longitudinal stiffeners, longitudinal stiffeners connecting outer and inner hull plating, inner hull longitudinal stiffeners, and deck stiffeners. Structural elements are made of several steel grades (A, B, AH) and have walls of different thickness values, ranging from 11 to 18.5 mm.

### 3.3 Boundary conditions

The fluid-structure interaction was not taken into account, and the collision was modelled as a pure deformable structure-rigid structure interaction. Hence, we can find the energy dissipated by the friction between both ships and by the plastic deformations, but not by the surrounding water.

The boundary conditions are applied at 4 planes:

- a) at two vertical bounding planes, the first one in the front and the second one in the rear of the model,
- b) at two vertical planes, cutting off the deck and the bottom parts.

For nodes belonging to the aforementioned planes all 3 displacement components were set to zero.

### 3.4 Material data of the struck ship

Elastic properties: Young's modulus  $E=210\text{GPa}$ , Poisson's ratio  $\nu=0.3$ . Density  $\rho=7800\text{ kg/m}^3$ . Two plastic material characteristics were applied:

**M1** Elastic-perfectly plastic model for steel. This idealised model satisfies the minimal value of the yield stress specified by the DNV Classification Rules, but uses a lower value of the ultimate plastic strain.

**Mild steel (Grade A, B):** Yield stress  $\sigma^Y=235\text{ MPa}$ , no hardening, ultimate plastic strain equal 0.1

**H.T. steel (Grade A):** Yield stress  $\sigma^Y=315\text{ MPa}$ , no hardening, ultimate plastic strain equal 0.1

**M2** Elastio-plastic with hardening model for steel. This model has been based on the experimental curves for tension. The tests results were obtained on the closed loop servo-hydraulic universal testing machine MTS810 (performed by Dr G. Socha of the IFTR PAS, Warsaw). The steel was manufactured in Italy and Finland.

The steel characteristics **M2** have been derived from the experimental curves such that:

- the yield stress  $\sigma^Y$  has the same (minimum) value as specified by DNV Classification Rules.
- the ultimate plastic strain is equal to 0.17, as specified by DNV Classification Rules, and obtained in the experiments.
- the shape of the stress - strain curve is similar to the experimental curve.

**Mild steel (Grade A, B):** Yield stress  $\sigma^Y=235\text{MPa}$ , tensile strength  $R_m = 400\text{ MPa}$ , ultimate plastic strain equal 0.17

**H.T. steel (Grade A):** Yield stress  $\sigma^Y=315\text{ MPa}$ , tensile strength  $R_m = 440\text{ MPa}$ , ultimate plastic strain equal 0.17

Material characteristics, i.e. the stress-strain curves, for **M1** and **M2** as well as the experimental curves are shown in Fig. 2.

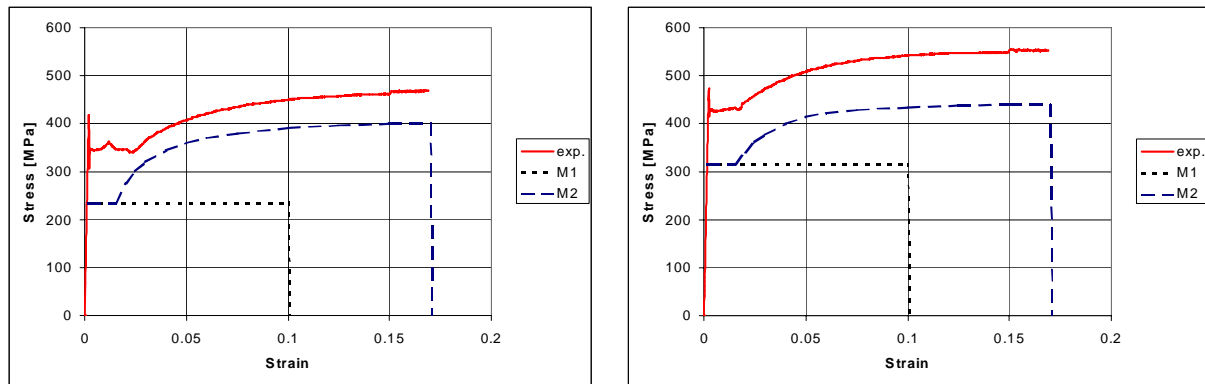


Fig. 2: Constitutive curves for (a) mild steel, and (b) H.T. steel

### 3.5 Contact definition

Details of the contact definition assumed by the authors are specific to the FE code used. Two following types of contact have been considered.

**C1** Contact of the striking bow, treated as a rigid surface, and a set of nodes of the struck ship. This type of contact was included in all analyses.

**C2** The contact within the interior of the double-hull of the struck ship. Due to a large distance between the inner and outer plating as well as a relatively small value of the ultimate plastic strain this type of contact was not physically important and therefore finally not accounted for.

Friction was taken into account for **C1**, and the following values of the friction coefficient were used: 0.0, 0.1, 0.3 and 0.6.

## 4 Numerical analyses and reference results

Ten analyses have been performed for the defined FE models of colliding ships, allowing to establish the influence of various parameters. The reference results provides the analysis **A4**, which has been performed for the material **M1**, the friction coefficient equal 0.6 for contact **C1**, the displacement boundary conditions, and no mass scaling.

### 4.1 Crushing force versus bow penetration

The 2<sup>nd</sup> law of Newton's dynamics,  $F=ma$ , has been employed to calculate the crushing force from the mass and the decelerations of the striking rigid bow provided by the FE program. The deceleration has been monitored for all time steps, the number of which exceeded 150 000; this number has been reduced by an automatic selection by the moving average to about 1000 points.

It can be observed (see Fig. 3) that the crushing force gradually increases with the penetration, which indicates that the striking bow decelerates at this stage more than at the beginning of the collision. Besides, the curve has many local ups and downs, which can be caused not only by complexity of the deformation process, but also by numerical effects such as:

- removal of the finite elements in which the ultimate plastic strain is exceeded in all Gauss points, and

- the contact algorithm, which exploits only a set of discrete points for the struck ship.

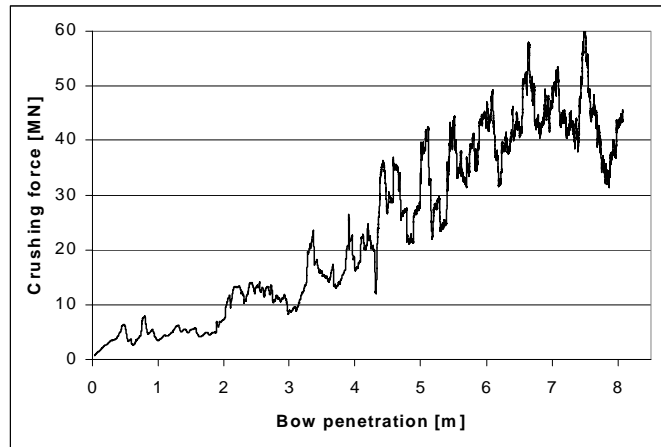


Fig. 3: Crushing force vs. bow penetration for **A4**

#### 4.2 Energy transformation

It can be seen from Fig. 4, that a sum of the strain, frictional and kinetic energy remains equal to the initial kinetic energy, which indicates that the numerical algorithm properly conserves the energy. The kinetic energy decreases, and this is compensated by an increase of the strain and frictional energies.

The strain energy consists of the following parts: the plastic energy, which is the highest one, the elastic energy, which is negligible, and the “artificial” energy associated with stabilisation of singular modes of the FE model.

The energy curves are smooth because they have been produced using of only the displacement and velocity, unlike the crushing force, which has been based on the deceleration.

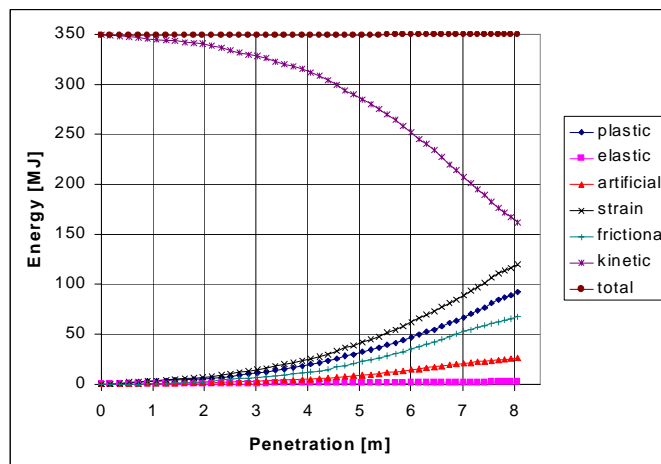


Fig. 4: Energy vs. bow penetration for **A4**

#### 4.3 Struck ship deformation

Fig. 5 depicts the struck ship final deformation. All the elements, for which the ultimate plastic strain measure has been exceeded in all Gauss points, have been removed from the model. It can be noticed that, after the element removal, the hole in the struck ship closely resembles the geometry of



the rigid bulbous bow. Also the deck indentation is similar to the shape of the upper part of the striking bow.

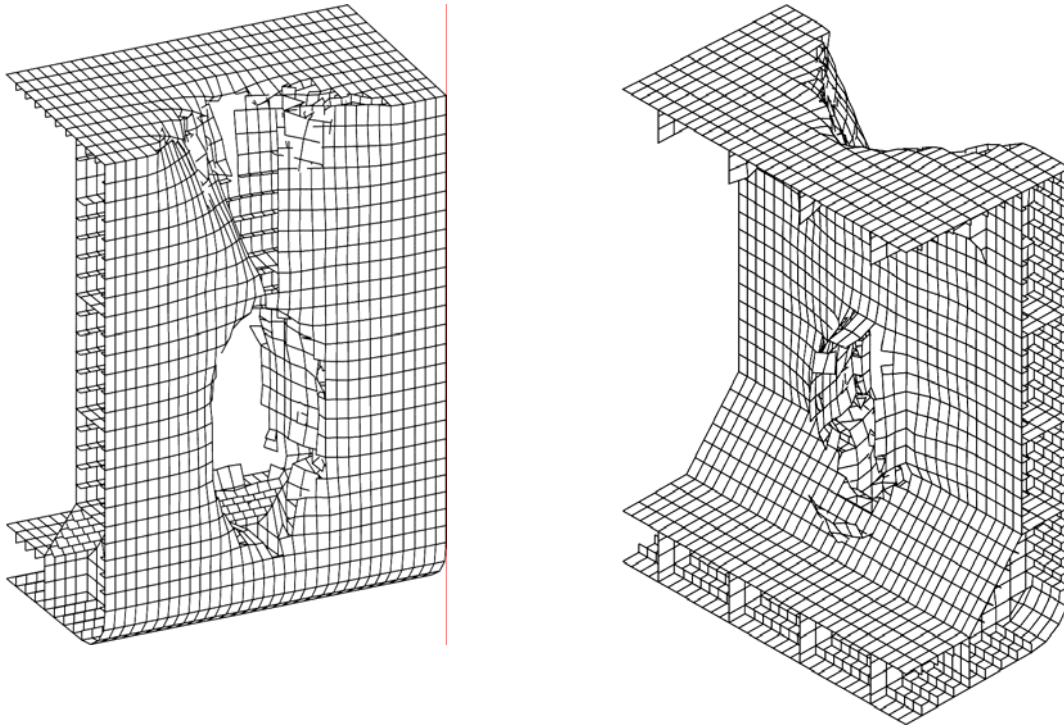


Fig. 5: Damage of struck ship after impact for **A4**

In these figures some of the elements are not connected to the main part, i.e. are “flying”, which is the result of a removal of their adjacent elements where an excessive plastic strain occurred. Such “flying” parts are a normal phenomenon in the explicit codes, and are used e.g. to model the trajectories of disrupted parts after a blast.

## 5 Influence of selected parameters on analysis results

Comparisons of results of analyses **A1-A10** allow us to evaluate influence of selected parameters, such as: the material characteristics, boundary conditions, friction coefficient, mass scaling, initial velocity of the striking ship, additional velocity component.

### 5.1 Mass scaling

The so-called mass scaling is a numerical technique designed to enlarge the length of time steps, and speed up computations. The larger is the mass scaling factor the higher speed up ratio is obtained. However, this technique is acceptable only when its influence on results is minor.

This technique has been applied with the mass scaling factor equal 100, which gives the speed up ratio equal 10. Next, for comparison, the analysis without the mass scaling has been carried out. It turned out that the mass scaling significantly affects the kinetic, strain and plastic energy as well as the crushing force.

## 5.2 Boundary conditions

Two types of the boundary conditions have been applied at the nodes along the struck ship model edges in the front, rear, bottom and deck part: either all displacements or all displacements and rotations were suppressed. The obtained results indicate that the crushing force is insensitive to the boundary condition types checked. A similar conclusion is true for the energies. Hence, only the boundary displacements have been suppressed in further analyses.

## 5.3 Friction coefficient

It has been difficult to assess the exact value of the friction coefficient, therefore a parametric study for the values equal 0.0, 0.1, 0.3 and 0.6 was performed. To separate the effect of the friction coefficient, the same values of the other parameters have been used.

Fig. 6 shows that the higher friction coefficient is, the faster loss of kinetic energy is observed. This result is in accord with the engineering intuition, which says that the friction speeds up the process of energy dissipation in any impact/contact process. It can also be seen that the difference between the curves for 0.3 and 0.6 is much smaller than between the curves for 0.0 and 0.3, hence, it can be expected that the effect of the friction will not increase significantly for larger values of the coefficient.

In Fig. 7 it can be seen that, in comparison to the case with no friction, the crushing force significantly increases when the friction coefficient equal to 0.6 is applied.

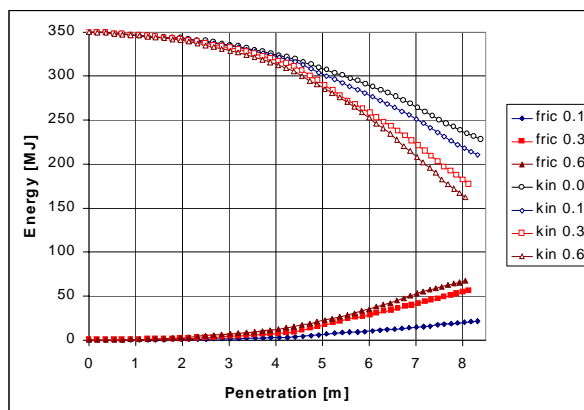


Fig. 6: Influence of friction coefficient on energy

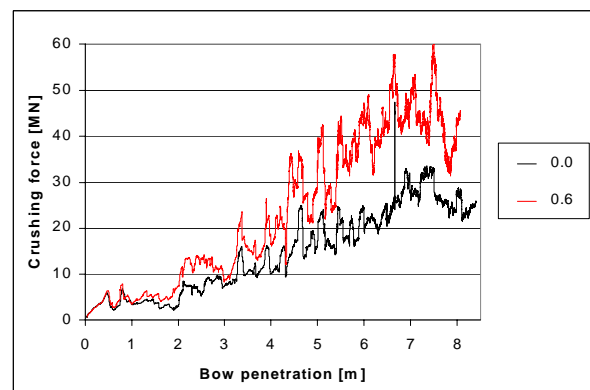


Fig. 7: Influence of friction coefficient on crushing force

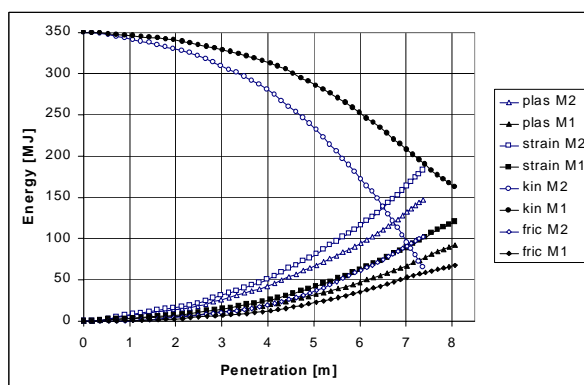


Fig. 8: Energies for M1 and M2

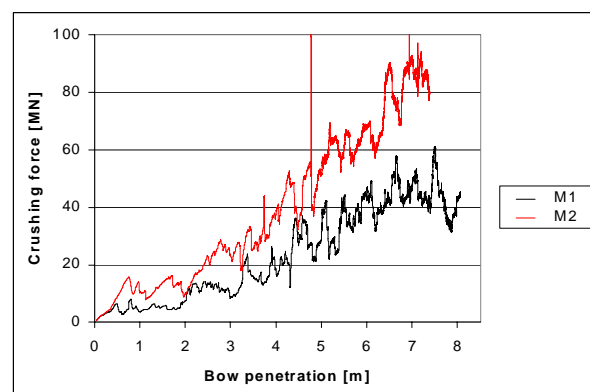


Fig. 9: Crushing force for M1 and M2



It can be concluded, that **M1** is quite conservative in comparison with the experiment-based **M2**. As current FE codes admit constitutive curves of a complicated form, it seems rather reasonable to use the experimental curves similar to **M2** in FE calculations, and control safety via a separate factor.

Similar tendencies can be observed for the case with no friction, though the kinetic energy decreases faster in the presence of friction.

#### 5.4 Velocity of Y-direction of the striking ship

The Y-direction is parallel to the longitudinal axis of the struck ship, and is perpendicular to the striking ship motion used in other analyses. The striking ship has a velocity of 7 knots in X-direction, and 3.5 knots in Y-direction. The Y-component of the velocity has been introduced in order to evaluate the effect of the struck ship motion in the simplest possible way. The simplification in this analysis consists in assigning the Y-component of velocity to the striking ship, instead of the struck ship. Note that it is not indifferent, which ship this additional velocity is assigned to, because the struck ship has 2.5 times bigger mass.

The orientation of the striking bow has remained unchanged, and has been kept normal to the longitudinal axis of the struck ship throughout the whole analysis.

The results of the analysis with the additional velocity in Y-direction and the analysis without it, are compared in Fig.10 and 11. The X-component of the crushing force, depicted in Fig. 10 is generally smaller for the analysis with the additional velocity component. Consequently, the deceleration is slower, and also the loss of kinetic energy shown in Fig. 11 is slower. This is likely to be due to the fact that the contact between both ships is now maintained only at one side of the striking bow, while at the other a widening gap occurs. Hence, it can be expected that the depth of penetration will be greater for the case with the additional velocity component. This also indicates that the case when the struck ship is not moving and remains still, is not the worst case in terms of the expected damage.

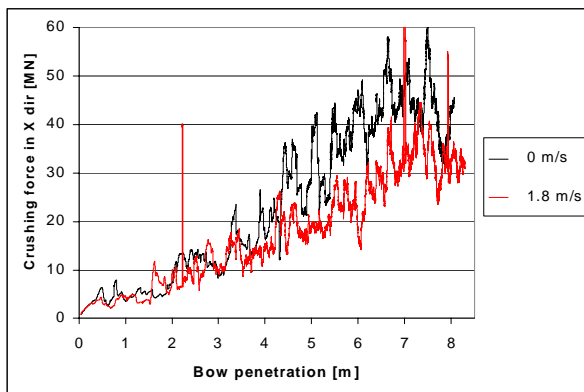


Fig. 10: Influence of velocity in Y-direction on crushing force in X-direction

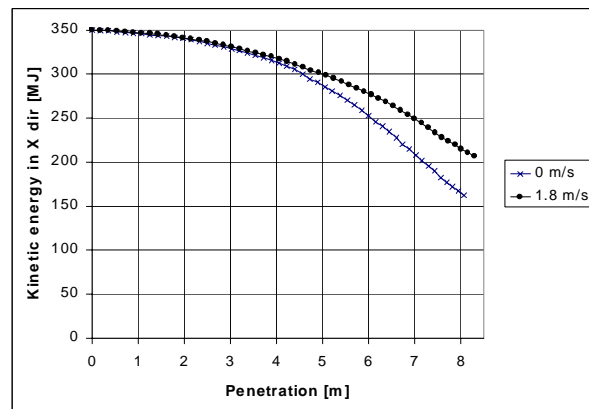


Fig. 11: Influence of velocity in Y-direction on kinetic energy in X-direction

#### 5.5 Initial velocity

The initial velocity in the reference analysis **A4** has been 7 knots (3.6 m/sec), and the analysis has been carried out until about the 8-meter indentation of the struck ship has been obtained, i.e. for about 2.5 seconds.

For comparison, the initial velocity of the striking ship has been reduced from 7 to 5 knots (2.57m/sec), which reduced the initial kinetic energy almost two times, from 350 to 178 MJ. Besides, the process has been slower in time, and the analysis has been run longer, for 5 seconds after the impact. Hence, at the end of analysis, the final velocity was equal to zero, while in the reference analysis **A4** it has

been about 2.5m/sec. In this way, for the friction coefficient equal 0.6, the moment when the whole kinetic energy was dissipated by the plastic deformation and friction has been captured.

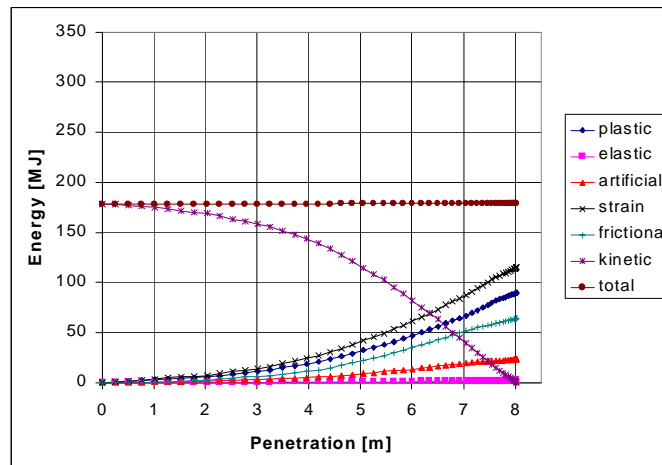


Fig. 12: Energies for initial velocity equal 5 knots

It is interesting to see in Fig. 12 that, from the moment when half of the kinetic energy is dissipated, i.e. for the 6-meter penetration, the kinetic energy curve almost linearly decreases to zero. It reaches zero at the 8-meter penetration, i.e. when in **A4** only half of the energy is dissipated. Assuming a similar character of the kinetic energy curve for **A4**, one can predict that then the maximum penetration, at which the striking ship stops, should be about 11 meters.

The dynamics of the collision has been different in both analyses, but comparing the crushing force vs. penetration curves, only small differences between these curves have been identified, which indicates that the deceleration/penetration ratio is similar. Also the energy dissipated in these analyses, shown as functions of the penetration, are almost the same. This confirms that by relating the different dynamic processes to the penetration we can compare them in a meaningful way.

## 6 Conclusions

The obtained results have been discussed in detail in the previous sections while here some additional comments are made, having in mind future simulations of ship collisions.

### 6.1 Striking ship velocity

- In presented computer simulations, the striking bow has been treated as rigid, which has been very convenient, because the number of degrees of freedom of a rigid bow was reduced to 6. However, its geometry has been almost exactly represented, which rendered that the contact between the ships and the damage of the struck ship has been quite realistically modelled.
- The results indicate a need for an exact initial velocity data for the striking ship, because it has a great influence on the extent of damage of the struck ship, as the kinetic energy depends on velocity square.
- It is shown that both velocity components are important, not only the normal to the direction of the struck ship motion. The tangent velocity changes significantly the collision process, as then the contact between both ships is maintained only at one side of the striking bow. In consequence the kinetic energy dissipation is slower, so one can expect a bigger hole and a deeper penetration.

## 6.2 Material model for struck ship

- The results show that large deformations and plastic strains dominate in the struck ship, while the elastic energy is negligible. Hence, constitutive modelling of the plastic part is essential, and two models were compared: the simple **M1**, suggested by the DTU, and the experiment-based DNV-compliant model **M2**. The conclusion is that **M1** is quite conservative in comparison with **M2**; e.g. the plastic energy is two times smaller for **M1**, which is equivalent to the safety factor equal 2.
- Current FE codes admit complicated constitutive curves, which can be specified as piece-wise linear functions. Hence, one can use in FE computations the experimental curves, similar to **M2**, and control safety via a separate factor.
- Peaks of the deceleration and the crushing force curves are generated by two features of the FE model: (a) the finite elements with the excessive plastic strains are removed from the model, which is essential for modelling of tearing (b) the contact is defined for a finite set of nodes of the struck ship. In both cases, a finer mesh and smaller elements can reduce these peaks.

Finally, it should be noted that though a dynamic FE code has been used, the crushing force and the dissipated energy are presented as functions of the rigid bow penetration and hence the relevant plots can be compared with results of a static analysis, for which the bow displacement is an independent parameter.

## 7 References

- [1] Lenselink, H. and Thung K. G., 1992. "Numerical simulations of the Dutch-Japanese full scale ship collisions tests". The MacNeal-Schwendler Company report, Gouda, The Netherlands.
- [2] Pedersen, P. Terndrup and Zhang, S., 2000. "Absorbed energy in collision and grounding – revising Minorski's Empirical Method", Journal of Ship Research, Vol. 44, No. 2, June, pp. 140-154.
- [3] Santosa, S. and Wierzbicki, T., 1998. "Crash behaviour of box columns filled with aluminium honeycomb and foam", Computers and Structures, Vol.38, pp.343-367.
- [4] Simonsen, B.C. and Ockali, H., 1999. "Experiments and Theory on Deck and Girder Crushing", Thin-walled Structures, Vol 34, pp. 195-216.
- [5] Simonsen, B.C., 2000. "Basic Modelling Principles and Validation of Software for Prediction of Collision Damage", ISES Report no. I108.02.02.052.004, Department of Naval Architecture and Offshore Engineering, Technical University of Denmark, April.
- [6] Wierzbicki, T., 1983. "Crushing Behaviour of Plate Intersections". Structural Crashworthiness, ed. by N. Jones and T. Wierzbicki, Chapter 3, Butterworth & Co. Publishers Ltd.
- [7] Wierzbicki, T., 1995 "Concertina Tearing of Metal Plates", Int. J. Solids Structures, Vol. 32, No. 19, pp. 2923-2943.